# Continuous Testing of Silica-PEI Adsorbents in a Lab.-Scale Twin Bubbling Fluidized-Bed System

Jae-Young Kim[a], Je-Min Woo[a], Sung-Ho Jo[a], Seung-Yong Lee[a], Jong-Ho Moon[a], Hyunuk Kim[a], Chang-Keun Yi[a], Hyojin Lee[a], Colin E. Snape[b], Lee Stevens[b], Chengong Sun[b], Hao Liu[b], Jingjing Liu[b] and Young Cheol Park[a,†]

[a]*Korea Institute of Energy Research, 152 Gajeong-ro, Yuseong-gu, Daejeon 34129, Republic of Korea*

[b]*University of Nottingham, Faculty of Engineering, The Energy Technologies Building, Triumph Road, Nottingham, NG7 2TU, UK*

## Abstract

In this study, a lab.-scale twin bubbling fluidized-bed system (TBS) has been used continuously to test the performance for $CO_2$ adsorption of silica-PEI (S.PEI) adsorbents, containing 40 wt.% of PEI, which were supplied by the University of Nottingham (UNOTT). The TBS comprises bubbling-bed adsorption and desorption reactors, a riser for pneumatic conveying of solids from the adsorption to the desorption reactor, and a cyclone for solid-gas separation. The adsorbent prepared using PEI with a molecular mass of 800 (S.PEI-0.8K) was a preliminarily tested for almost 24 hours at the given operating conditions by varying the inlet sorbent/$CO_2$ mass ratio at the adsorber to analyse the $CO_2$ removal efficiency in the adsorption reactor and the dynamic sorption capacity of the adsorbent. A 180-hour continuous test was then carried out by changing various experimental conditions such as the $H_2O$ concentration, reaction temperature, solid layer height, reaction gas flow rate, and inlet sorbent/$CO_2$ mass ratio at the adsorber using PEI with a molecular mass of 5000 (S.PEI-5K) adsorbent. In this test, a $CO_2$ removal efficiency of above 80% and a dynamic sorption capacity greater than 6.0% were achieved.

---

[†] To whom all correspondence should be addressed. E-mail: youngchp@kier.re.kr

Keywords: Post-combustion $CO_2$ capture; Dry solid sorbent; silica-PEI adsorbents; Lab.-scale twin bubbling fluidized-bed system; Continuous performance test

## 1. Introduction

In an effort to address the global climate change issues, the international environmental regulations on greenhouse gases have been strengthened, and the need for environmental technology development has been emphasized. $CO_2$ emissions account for approximately 88% of greenhouse gas emissions and a large part of $CO_2$ emissions come from fixed sources such as power plants using fossil fuels (Joen and Sa, 2010; White et al., 2013). $CO_2$ concentration in the atmosphere has exceeded 400 ppm and is estimated to increase to over 500 ppm by 2050 in case without actions, which will increase the global average temperature (IPCC, 2013). Since the operation of power plants using fossil fuels is expected to operate continuously in the future, strategies to reduce the $CO_2$ concentration are necessary (D'Alessandro et al., 2010; Haszeldine, 2009). Recently, much attention has been given of late to the economical and environment-friendly carbon capture, utilization and storage (CCUS) technology for collecting the emitted $CO_2$ from thermal power plants. The implementation of CCUS technology in power plants has been proposed as a means to enable the continuous use of fossil fuels in the short term. In particular, post-combustion $CO_2$ capture is drawing significant attention because it is easily applicable to existing power plants (D'Alessandro et al., 2010; Haszeldine, 2009).

Among the various approaches to $CO_2$ capture, post-combustion $CO_2$ capture using amine aqueous solution has been researched intensively and has been used in industries for over five decades (D'Alessandro et al., 2010; Rochelle, 2009). However, the process using amine aqueous solution has several limitations, including high energy demand for and environmental problems such as volatile amine loss and reactor corrosion (Nguyen et al., 2010; Figueroa et al., 2008). To overcome these limitations, non-corrosive dry solid particles with a low regeneration energy penalty have been proposed as potential alternatives to liquid adsorbents (Choi et al., 2009; Bollini et al., 2011; Wang et al., 2014). In particular, technology using dry solid particles is currently being researched on as an innovative concept for $CO_2$ capture and recovery. Various solid adsorbents have been researched, including adsorbents based on carbonates such as sodium, potassium, and calcium (Liang et al., 2004; Lee et al., 2008; Fang et al., 2009; Lee et al., 2011), zeolites (Shang et al., 2012), carbons (Hao et al., 2011), metal‒organic frameworks (MOFs) (Mason et al., 2011; Chaikittisilp et al., 2011), and amine-modified porous materials (Kim et al., 2016; Choi et al., 2016; Min et al., 2017, 2018). In particular, amine-modified adsorbents have been researched extensively because they can effectively $CO_2$ adsorption in exhaust gases containing vapors.

However, few studies on the post-combustion $CO_2$ capture with amine-modified adsorbents at pilot-scale process have been reported. ADA Environmental Solution (ADA-ES) has developed a new concept reactor by incorporating staged fluidized beds for adsorption and a single fluidized bed for regeneration to take advantage of the properties of functionalized amines sorbent. ADA-ES has performed studies on $CO_2$ capture in a 1 MWe-scale process, and reported that the amine adsorbent can achieve 90% $CO_2$ capture. (Krutka et al., 2013; Morris et al., 2014). Research Triangle Institute (RTI) has developed an advanced solid sorbent-based $CO_2$ capture process for application to exhaust gas from various industrial sources including coal-fired power plants, NGCC power plants, and cement plants. RTI International has performed a bench-scale demonstration tests and economic analyses related to diverse $CO_2$ emission sources using a sorbent material that is based on a poly-amine (PEI) loaded on a silica initially developed at Pennsylvania State University. (Nelson et al., 2017). The University of Nottingham (UNOTT) has developed polyethyleneimine (PEI)-based sorbent for post-combustion $CO_2$ capture (Drage et al., 2008, 2012). Zhang et al. evaluated using a laboratory-scale bubbling fluidized bed reactor loaded with a few kg adsorbent, the adsorption performance of PEI–silica adsorbent under different working conditions including with and without the presence of moisture, different gas–solid contact times, initial bed temperatures, and $CO_2$ partial pressures (Zhang et al., 2014). In addition, Zhang et al. evaluated the most important parameters affecting the regeneration heat, including the physical properties of the adsorbents and process related variables including the heat of adsorption, specific heat capacity, working capacity, moisture adsorption of the PEI-silica adsorbent, the swing temperature difference and the degree of heat recovery. They also estimated the working capacity of the PEI-silica adsorbent using pseudo-equilibrium capacities obtained from the isobaric TGA tests (Zhang et al., 2016). KIER has developed dry $CO_2$ capture technology using solid sorbents, and related research is being conducted. The research results on $CO_2$ capture in a laboratory-scale device have been steadily reported, and a pilot-scale $CO_2$ capture process using dry adsorbents has been developed, consisting of a fluidized-bed-type adsorption reactor and a regeneration reactor (Yi et al., 2007, 2008; Yi, 2009, 2010; Park et al., 2009a,b, 2011; Kim et al., 2010, 2011). At present, the authors are continuing their research using dry adsorbents, and are developing more economical and energy-efficient dry adsorbents and the $CO_2$ capture process for commercial scale of 10 MWe (Park et al., 2013, 2014a,b, 2016; Kim et al., 2017).

In this study, experiments were conducted to evaluate the $CO_2$ capture performance of silica-PEI adsorbent in a laboratory-scale twin bubbling fluidized-bed system (TBS). A 24-hour preliminary test and 180-hour continuous operation were performed using two types of adsorbents with different PEI molecular masses, and the $CO_2$ capture performance of the adsorbent was evaluated.

## 2. Experimental

### 2.1 Physical properties of materials

The silica-PEI sorbent used in this study was prepared by UNOTT by impregnating a mass fraction of 40 wt.% PEI into a commercial mesoporous silica support. In the experiments, two types of silica-PEI adsorbents with different PEI molecular masses were used. Table 1 summarizes the PEI molecular mass, bulk density, average particle size, particle size distribution and the attrition index.

(Table 1)

The bulk density of the silica-PEI adsorbent was measured using a measuring cylinder, and the average value of five measurements was used. The attrition of the solid particles was measured with a fluidized bed particle attrition test system according to the method of American Society for Testing and Material (ASTM) D5757-95. The particle attrition was indicated using an attrition index (AI), which was calculated based on the solid loss rate by attrition after 5 hours (AI(5)). The average particle size and particle size distribution (PSD) of silica-PEI adsorbents were verified using a particle size analyzer (S3500, Microtrac) and the average value of three measurements was used.

### 2.2 Apparatus

A schematic diagram of the TBS used in this study is shown in Fig. 1. The rig consists of bubbling fluidized-bed type adsorption and desorption reactors, a transport tube for recycling the solid particles after adsorption, a cyclone for separating the gas and solid, a rotary valve for adjusting the solid circulation amount, and an infrared (IR) gas analyzer (ABB, Advance Optima) for measuring the gas concentrations before and after the reaction.

The adsorption and desorption reactors were fabricated as bubbling fluidized-beds with a 0.1 m inner diameter and a 1.0 m height. An air box with a perforated-plate-type gas distributor was installed at the bottom of the reactor, and, for circulating the solid particles, an overflow type was fabricated. A heater was installed outside the air box of each reactor to prevent partial cooling inside the reactor (the gas inlet part), thus minimizing the temperature difference between the injected gas and the inside of the reactor. A temperature control device was installed outside each reactor, and a jacket-type heat exchanger was installed outside the adsorption reactor. A cooling water with an adjusted temperature in the cooling water supplier (auto chiller, HYUNDAI ENGCO., LTD., Korea) was supplied to the heat exchanger to adjust the temperature of the reactor and to control the heat generated from the adsorption reaction. A heater was installed outside the desorption reactor to heat the reactor and control the reaction temperature. The simulated gas was used for the gas supplied to each reactor, and a device for injecting $H_2O$ was installed in front of each reactor. For the reaction gas of the adsorption reactor, the simulated gas with a mixture of $N_2$ (99.99%), $CO_2$ (99.9% or higher), and $H_2O$ was used. A bubbler was installed before the adsorption reactor to generate vapor, which is required for simulating coal-fired flue gas condition. A line heater was installed in the gas inlet pipe at the back of the bubbler to prevent water condensation in the inlet gas. For the fluidizing gas supplied to the desorption reactor, the simulated gas with a mixture of $N_2$ (99.99%) and $H_2O$ was used. A water pump was installed before the desorption reactor to inject moisture and adjust the amount of moisture flowing into the reactor. In addition, a pre-heater was installed to heat the gas and vaporize the inflow liquid-state $H_2O$. A heater was installed outside the desorption reactor to heat the reactor and control the reaction temperature.

The transport tube for the solid particles was fabricated as a fast fluidized bed with a 0.02 m inner diameter and a 4.0 m height. For the gas supplied to the transport tube, $N_2$ (99.99%) was used. A pre-heater was installed before the transfer device to increase the temperature of the gas and to prevent the cooling of the solid particles coming from the adsorption reactor. The gas flowing into the transport tube transfers the solid particles to the main cyclone, which separates gas and solid and supplies solid particles to the desorption reactor. For the gas injected into each reactor, the concentration of the reaction gas ($CO_2$) and the inflow rate of the reactor were adjusted using a mass flow controller (E5850, Brooks Instruments). Rotary valves were installed at the bottom of the adsorption reactor, desorption reactor, and main cyclone. The circulation rate of the solid particles was adjusted using the rotary valve. Resister temperature detectors (RTDs) were installed in each reactor, gas pipe, etc. The temperature of each point was measured, and the temperatures of the reactor (or adsorbent) and gas were detected using the RTD. Furthermore, the adsorbent and gas flow conditions were examined by installing a pressure gauge and a differential pressure gauge. The humidity of the gas was measured using a thermo-hygrometer (C-310 multifunction sensor, KIMO INSTRUMENTS, France) at the reactor inlet and outlet, and the humidity values measured before and after the reaction were compared. Furthermore, an IR gas analyzer was installed to measure the gas ($CO_2$) before and after the reaction. The measurements values obtained from the instruments (thermometer, differential pressure gauge, analyzer, etc.) installed in the TBS were collected through a Programmable Logic Controller (PLC) and were stored in the computer.

(Fig. 1)

## 2.3 Experimental conditions and method

A preliminarily test in the TBS was performed using the S.PEI-0.8K adsorbent, and a 180-hour continuous test was then performed using S.PEI-5K adsorbent. The flow rate of the gas flowing into the adsorption and desorption reactors was set to 4.5 cm/s. Solid particles initially charged into two reactors and they flow into the adsorption reactor from the desorption reactor when solid circulation started. The solid particles flowing into the adsorption reactor flow into the transport tube after the adsorption reaction. Those scattered in the transport pipe are captured in the main cyclone and are recirculated to the desorption reactor. The solid circulation rate is determined by the rotation speed of the rotary valve installed between the desorption reactor and the adsorption reactor. After setting the rotation speed of the rotary valve installed between the desorption and reactors, when the other two rotary valves were stopped, the solid circulation rate was calculated using the differential pressure value for the adsorption reactor which changes with time and the bulk density of adsorbents. During the solid circulation, the desorption reactor was heated to the desorption reaction temperature (128-130°C). Before the continuous tests, the solid particles were dried and regenerated for approximately 12 hours at the temperature of 130°C and at a solid circulation rate of 4.20 kg/h. The continuous test was then started. During this test, the gases at the inlet and outlet of the adsorption reactor and the outlet of desorption reactor were measured by an IR gas analyzer. The amount of $CO_2$ adsorption and the $CO_2$ removal efficiency were calculated using the $CO_2$ concentration measured by an IR gas analyzer at each point. The dynamic sorption capacity was calculated based on the amount of $CO_2$ adsorption and the solid circulation rates. The samples after the reaction were collected from the bottom of the reactor. The samples collected after the reaction were compared with the samples before the reaction in terms of average particle size and PSD.

### *2.3.1 Preliminarily test*

The experimental conditions used for the preliminary test using S.PEI-0.8K are summarized in Table 2. For the inlet gas of the adsorption reactor, the simulated gas with a mixture of $N_2$ and $CO_2$ was used. As a fluidizing gas, $N_2$ was injected into the desorption reactor. The experimental conditions of the adsorption reactor were set as follows: inlet $CO_2$ concentration of 15 vol.%, reaction temperature of 70°C, and differential pressure in the reactor of 300 mm$H_2O$. Those of the desorption reactor were set as follows: reaction temperature of 130°C and differential pressure in the reactor of 300 mm$H_2O$. And then, the $CO_2$ capture performance of the S.PEI-0.8K adsorbent were examined according to the inlet sorbent/$CO_2$ mass ratio at the adsorber.

(Table 2)

### *2.3.2 180-hour continuous test*

The 180-hour continuous test was performed in the TBS to evaluate the $CO_2$ capture performance of the S.PEI-5K adsorbent with the goal to achieve above 80% $CO_2$ removal efficiency and above 6.0 wt.% dynamic sorption capacity. In order to determine the best operating conditions, several variables such as the $H_2O$ concentration at the inlet gas stream of both reactors, reaction temperatures, solid height of the adsorption reactor, and the inlet sorbent/$CO_2$ mass ratio at the adsorber have~~s~~ been considered. The experimental conditions used for the 180-hour continuous test are summarized in Table 3.

(Table 3)

The simulated flue gas mixture of $N_2$, $CO_2$ and $H_2O$ was used as the inlet gas for the adsorption reactor and a mixture of $N_2$ and $H_2O$ was used for the desorption reactor. The experimental conditions of the adsorption reactor were set as follow: inlet $CO_2$ concentration of 14.6 vol.%, inlet $H_2O$ concentration of 3.3 vol.%, reaction temperature of 65$^{o}$C, and differential pressure in the reactor of 300 mm$H_2O$. Those of the desorption reactor were set as follows: inlet $H_2O$ concentration of 5.0 vol.%, reaction temperature of 130$^{o}$C, and differential pressure in the reactor of 300 mm$H_2O$. Furthermore, the solid circulation rate was set to 3.89 kg/hr. The operating conditions were changed to achieve optimal performance. To examine $H_2O$ adsorption and the desorption behavior of the S.PEI-5K adsorbent, the $H_2O$ injection to the desorption reactor was stopped, and the concentration of the $H_2O$ introduced to the adsorption reactor was increased. When the $H_2O$ injection was stopped, the effect of adsorption temperature on $CO_2$ capture performance was investigated by decreasing the temperature to 65, 60, and 55$^{o}$C. The effect of the solid height of the adsorption reactor on $CO_2$ capture performance at the adsorption reactor temperature of 55$^{o}$C was also investigated. The differential pressure of the adsorption reactor, which directly related with the solid bed height, was decreased to 300, 255, and 220 mm$H_2O$. The differential pressure of the adsorption reactor was controlled by varying discharge rate of solid particles. Because of the reactor shape, the minimum differential pressure of the reactor was 220 mm$H_2O$ when solid circulation is possible. After the solid height variation test, the adsorption and desorption reactors were operated with differential pressures of 300 and 250 mm$H_2O$, respectively. After that, the temperature of the adsorption reactor was set to 65$^{o}$C, and the effect of the solid circulation rate on $CO_2$ capture performance was investigated. Finally the temperature of the desorption reactor was decreased from 130 to 120$^{o}$C after setting the solid circulation rate of 3.89 kg/hr so the effect of desorption temperature on $CO_2$ capture performance could be investigated.

## 3. Results and Discussion

### 3.1 Preliminarily test

Fig. 2 shows a preliminary test results using the S.PEI-0.8K adsorbent, presenting the $CO_2$ removal efficiency and the dynamic sorption capacity according to the inlet sorbent/$CO_2$ mass ratio at the adsorber. The calculation of the $CO_2$ removal efficiency and the dynamic sorption capacity is as follows:

$$\text{The CO}_2\text{ removal efficiency (\%)} = 1 - \frac{\text{outlet CO}_2\text{ mole flow rate at the adsorption reactor (kmol/hr)}}{\text{intlet CO}_2\text{ mole flow rate at the adsorption reactor (kmol/hr)}} \times 100 \quad (1)$$

$$\text{The dynamic sorption capacity (wt.\%)} = \frac{\text{captured CO}_2\text{ mass flow rate at the adsorption reactor (kg/hr)}}{\text{solid circulation rate (kg/hr)}} \times 100 \quad (2)$$

The inlet sorbent/$CO_2$ mass ratio at the adsorber is an important factor which affects the adsorption capacity of solid particles. Thus, it is crucial to find the effect of inlet sorbent/$CO_2$ mass ratio at the adsorber and the effect of solid circulation rate on the $CO_2$ removal efficiency and dynamic sorption capacity of the solid particles. The test results showed that the $CO_2$ removal efficiency was 72.5, 84.2, 92.7, and 95.0% and the dynamic sorption capacity was 6.36, 5.05, 3.08, and 2.20 wt.% at inlet sorbent/$CO_2$ mass ratio at the adsorber of 7.3, 10.6, 19.2, and 27.4, respectively. As the inlet sorbent/$CO_2$ mass ratio at the adsorber increased, the removal efficiency also increased, but the dynamic sorption capacity decreased. Based on this test, it is possible to achieve 80% of $CO_2$ removal efficiency and above 5.5 wt.% dynamic sorption capacity when the inlet sorbent/$CO_2$ mass ratio at the adsorber is between 7.3 and 10.6.

(Fig. 2)

### 3.2 180-hour continuous test

Fig. 3 shows the results of the 180-hour continuous test using the S.PEI-5K adsorbent in the TBS. Fig. 3(a) shows the $CO_2$ removal efficiency and inlet and outlet $CO_2$ concentration profiles of the adsorption reactor. During the 180-hour continuous test, the $CO_2$ was introduced at the specified concentration (14.6 or 15.2 vol.%) into the adsorption reactor. It can be seen that the outlet $CO_2$ concentration after adsorption has changed depending on the operating condition. From the beginning, 78~85% of $CO_2$ removal efficiency was maintained until 150 hours of continuous operation. After 150 hours, the $CO_2$ removal efficiency changed greatly from 73% to 88% according to solid circulation rate and desorption temperature. Fig. 3(b) shows the dynamic sorption capacity and solid circulation rate of the solid particles. Up to 150 hours of continuous operation, the dynamic sorption capacity was maintained around 6.0~6.5 wt.%. Further, after 150 hours, the dynamic sorption capacity changed greatly from a minimum of 5.54 wt.% to a maximum of 7.43 wt.% according to the changes in the solid circulation rate and desorption temperature. Fig. 3(c) shows the inlet and outlet $H_2O$ concentration profiles of the adsorption and desorption reactors. The $H_2O$ adsorption and desorption behavior of the solid particles were investigated during the continuous operation. $H_2O$ was introduced to the adsorption reactor at a 3.3 vol.% concentration, but after 60 hours of continuous operation, the $H_2O$ concentration increased above 6.5 vol.%. However, the outlet $H_2O$ concentration increased slightly because the amount of $H_2O$ adsorbed by the solid particles increased as the inlet $H_2O$ concentration to the adsorption reactor increased. The outlet $H_2O$ concentration was higher than inlet $H_2O$ concentration in the desorption reactor. Fig. 3(d) shows the temperature profiles of the adsorption and desorption reactors. During the 180-hour continuous operation, the temperatures of the adsorption and desorption reactors were maintained at the specified values. Fig. 3(e) shows the differential pressure profiles of the adsorption and desorption reactors. The differential pressures of the adsorption and desorption reactors were maintained at the specified values during the continuous operation.

(Fig. 3)

Up to 90 hours, the performance of the adsorbent did not change much even when the temperature of the adsorption reactor changed. Below 60°C, the $CO_2$ removal efficiency and the dynamic sorption capacity were maintained at 84.2% and 6.4 wt.%, respectively. The sorption capacity of the adsorbent was maintained very well at below 60°C, being consistent with coal-fired flue gas temperature (55-60°C) after flue gas desulfurization (FGD).

After 120 hours, the differential pressure of the adsorption reactor decreased to 300, 255, and 220 $mmH_2O$. The $CO_2$ removal efficiency and the dynamic sorption capacity of the adsorbent did not change much. The differential pressure of the reactor indicates the solid height, which is related to the gas-solid contact time of the adsorbent. As the differential pressure of the reactor increases, the solid bed height also increases, as well as, the gas-solid contact time of the adsorbent increases. The increase in the differential pressure of the reactor can improve the $CO_2$ capture performance of the adsorbent due to the increase in the ~~of~~ gas-solid contact time. Zhang et al. reported that an increase in gas-solid contact time can effectively increase the working capacity as well as increase the inventory bed mass in the reactor (Zhang et al., 2014). However, it seems that the solid height of the adsorption reactor had little effect on the $CO_2$ capture performance of the adsorbent in the 180-hour continuous test. The minimum differential pressure at which solid circulation is possible in the TBS is 220 $mmH_2O$. In the 180-hour continuous test, the gas-solid contact time is 7.5 seconds in case of differential pressure in adsorption reactor of 220 $mmH_2O$. In this continuous test, the $CO_2$ capture performance of the adsorbent did not changed significantly until the gas-solid contact time decreased to 7.5 seconds. In addition, it was confirmed that the $CO_2$ removal efficiency and the dynamic sorption capacity were maintained at both above 80% and 6.0 wt.%, respectively. Based on the test, this means that the adsorbent have a sufficient gas-solid contact time even at the minimum differential pressure condition in the TBS.

After 150 hours, the effect of the inlet sorbent/$CO_2$ mass ratio at the adsorber on $CO_2$ removal efficiency and the dynamic sorption capacity. Fig. 4 shows the results according to the inlet sorbent/$CO_2$ mass ratio at the adsorber. When the inlet sorbent/$CO_2$ mass ratio at the adsorber increased to 11.2, 12.2, 13.2, 14.2 and 15.2, the $CO_2$ removal efficiency increased to 83.2, 83.9, 84.2, 87.5 and 88.1%, but the dynamic sorption capacity decreased to 7.43, 6.88, 6.39, 6.20 and 5.81 wt.%, respectively. Below the inlet sorbent/$CO_2$ mass ratio at the adsorber of 14.2, it is capable of achieving both above 80% $CO_2$ removal efficiency and 6.0 wt.% dynamic sorption capacity. This demonstrates that the S.PEI-5K adsorbent has an excellent dynamic sorption capacity. Zhang et al. estimated the working capacity of a 40% PEI/silica adsorbent as 1.35 mmol/g (5.94 wt.%) using pseudo-equilibrium capacities obtained from the isobaric TGA tests (Zhang et al., 2016).

(Fig. 4)

Immediately before finishing the continuous test, the effect of the desorption temperature on the $CO_2$ removal efficiency and the dynamic sorption capacity was investigated. As shown in Table 4, the $CO_2$ removal efficiency and the dynamic sorption capacity at the 120°C desorption temperature were lower than those at the 130°C desorption temperature. The $CO_2$ capture performance falls due to extent of $CO_2$ desorption decreasing.

(Table 4)

### 3.3 Particle size distribution (PSD) before and after reaction

Fig. 5(a) shows the particle size distributions of the S.PEI-0.8K adsorbent before and after the preliminary test, this adsorbent having multiple peaks of PSD. The particle size distributions of S.PEI-0.8K adsorbent before and after the reaction were 28-592 ㎛ and 34-498 ㎛ respectively.

After the preliminary test, 510㎛ or larger particles were abraded and did not appear in the particle size distribution. Furthermore, the 320-500㎛ particles decreased, the 175-300㎛ particles increased, the 120-170㎛ particles decreased, and the 65-120㎛ particles increased. The particles smaller than 60 ㎛ were separated in the cyclone and discharged from the TBS and decreased greatly. Fig. 5(b) shows the PSD of the S.PEI-5K adsorbent before and after the 180-hour continuous test. This adsorbent has a uniform PSD giving a single maximum in the PSD. Before and after the continuous operation, the S.PEI-5K adsorbent displayed the same particle size distribution of 80-498 ㎛. After the continuous operation, the 320-500㎛ particles decreased significantly while the 175-300㎛ particles increased. and, the 170㎛ or smaller particles also decreased.

In this test, the change in the particle size distribution of the silica-PEI adsorbent is considered to be due to the attrition of the solid particles. When solid particles flow through the adsorption reactor to the solid transport tube, the flow rate of the gas increases greatly. Due to the increased flow rate of gas, collision of the solid particles constituting the fluidized bed occurs frequently. The 320-500㎛ particles showed the largest change in PSD, suggesting that the attrition of the particles in this size range is the largest. The attrition of particles generates fine particles, which are separated in the cyclone and discharged from the system. This is a factor causing particle loss in the process operation. The attrition loss of solid particles leads to an economic loss in the process operation. Therefore, considering long-term process operation, the S.PEI-5K adsorbent, which has a smaller distribution of 320-500㎛and smaller attrition index of 2.09, are considered more advantageous for the fluidized bed process than S.PEI-0.8K adsorbent.

(Fig. 5)

## 4. Conclusions

1) The preliminary test using the S.PEI-0.8K adsorbent showed that when the inlet sorbent/$CO_2$ mass ratio at the adsorber increased to 7.3, 10.6, 19.2, and 27.4, the $CO_2$ removal efficiency increased to 72.5, 84.2, 92.7, and 95.0%, while the dynamic sorption capacity decreased to 6.36, 5.05, 3.08, and 2.20 wt.%, respectively. It is possible to achieve 80% $CO_2$ removal

efficiency and 5.5 wt.% dynamic sorption capacity at the inlet sorbent/$CO_2$ mass ratio at the adsorber between 7.3 and 10.6.

2) The 180-hour continuous test using the S.PEI-5K adsorbent showed the $CO_2$ capture performance of adsorbent has been the $CO_2$ removal efficiency of 84.2% and the dynamic sorption capacity of 6.4% when temperatures in adsorption reactor of below 60°C. It was confirmed that the sorption capacity of the adsorbent was excellent at below 60°C adsorption temperatures.

3) In the 180-hour continuous test, a $CO_2$ removal efficiency of above 80% and a dynamic sorption capacity of above 6.0% were continuously maintained until the differential pressure of the adsorption reactor decreased from 300 to 220 $mmH_2O$. This means that S.PEI-5K adsorbent had a sufficiently long gas-solid contact time (7.5 sec) even at the minimum differential pressure condition (220 $mmH_2O$) in the TBS.

4) In the 180-hour continuous test, the $CO_2$ removal efficiency increased but the dynamic sorption capacity decreased when the inlet sorbent/$CO_2$ mass ratio at the adsorber increased. Below the inlet sorbent/$CO_2$ mass ratio at the adsorber of 14.2, it is capable of achieving both above 80% $CO_2$ removal efficiency and 6.0 wt.% dynamic sorption capacity.

5) In the 180-hour continuous test, the $CO_2$ removal efficiency and the dynamic sorption capacity decreased when the desorption temperature was decreased from 130 to 120°C due to less $CO_2$ being desorbed.

6) The particle size analysis results, confirmed a change in the particle size distribution after the test, due to attrition. In particular, the attrition of the 320-500㎛ particles was the largest. When long-term process operation using the silica-PEI adsorbent is considered, S.PEI-5K adsorbents, which have a smaller particle size distribution of 320-500 ㎛ and smaller attrition index of 2.09, appear to be appropriate for application to the fluidized bed process. These adsorbents can provide economic benefit in process operation considering the life cycle and attrition loss of solid particles.

## Acknowledgements

This work was supported by the Korea Institute of Energy Technology Evaluation and Planning (KETEP) and the Ministry of Trade, Industry & Energy (MOTIE) of the Republic of Korea (No. 20158510011280)

## References

Bollini, P., Didas, S. A., Jones, C. W., 2011. Amine-oxide hybrid materials for acid gas separations. Journal Materials Chemistry 21, 15100-15120.

Chaikittisilp, W., Kim, H. J., Jones, C. W., 2011. Mesoporous alumina-supported amines as potential steam-stable adsorbents for capturing $CO_2$ from simulated flue gas and ambient air. Energy & Fuels 25, 5528-5537.

Choi, S., Drese, J. H., Jones, C. W., 2009. Adsorbent materials for carbon dioxide capture from large anthropogenic point sources. ChemSusChem 2, 796-854.

Choi, W., Min, K., Kim, C., Ko, Y. S., Jeon, J. W., Seo, H., Park, Y.-K., Choi, M., 2016. Epoxide-functionalization of polyethyleneimine for synthesis of stable carbon dioxide adsorbent in temperature swing adsorption. Nature Communications 7, No. 12640.

D'Alessandro, D. M., Smit, B., Long, J. R., 2010. Carbon dioxide capture: prospects for new materials. Angewandte Chemie International Edition 49 (35), 6058–6082.

Drage, T. C., A. Arenillas, A., Smith, K. M., Snape, C. E., 2008. Thermal stability of polyethyleneimine based carbon dioxide adsorbents and its influence on selection of regeneration strategies. Microporous and Mesoporous Materials 116, 504–512.

Drage, T. C., Snape, C. E., Stevens, L. A., Wood, J., Wang, J., Cooper, A. I., Dawson, R., Guo, X., Satterley, C., Irons, R., 2012. Materials challenges for the development of solid sorbents for post-combustion carbon capture. Journal Materials Chemistry 22, 2815.

Fang, F., Li, Z., Cai, N., 2009. Continuous $CO_2$ capture from flue gases using a dual fluidized bed reactor with calcium-based sorbent. Industrial & Engineering Chemistry Research 48 (24), 11140-11147.

Figueroa, J. D., Fout, T., Plasynski, S., McIlvried, H., Srivastava, R. D., 2008. Advances in $CO_2$ capture technology−the U.S. department of energy's carbon sequestration program. International Journal of Greenhouse Gas Control 2, 9-20.

Haszeldine, R. S., 2009. Carbon capture and storage: how green can black be?. Science 325, 1647–1652.

Hao, G.-P., Li, W.-C., Qian, D., Wang, G.-H., Zhang, W.-P., Zhang, T., Wang, A.-Q., Scheth, F., Bongard, H.-J., Lu, A.-H., 2011. Structurally designed synthesis of mechanically stable poly (benzoxazine-co-resol)-based porous carbon monoliths and their application as high-performance $CO_2$ capture sorbents. Journal of American Chemical Society 133, 11378–11388.

International Panel on Climate Control (IPCC), 2013. Summary for Policymakers. In Climate Change 2013: The Physical Science Basis; Cambridge University Press. Cambridge, MA.

Jeon, E. C., Sa, J. H., 2010. Development of $CO_2$ emission factor by fuel and $CO_2$ analysis at sub-bituminous fired power plant. Journal of Environment Health Science 36(2), 128-135.

Kim, C., Cho, H. S., Chang, S., Cho, S. J., Choi, M., 2016. An ethylenediamine-grafted Y zeolite: a highly regenerable carbon dioxide adsorbent via temperature swing adsorption without urea formation. Energy & Environmental Science 9, 1803−1811.

Kim, J. -Y., Lim, H., Woo, J. M., Jo, S. -H., Moon, J. -H., Lee S. -Y., Lee H., Yi, C. -K. 2017. Performance evaluation of K-based solid sorbents depending on the internal structure of the carbonator in the bench-scale $CO_2$ capture process. Korean Chemical Engineering Research 55 (3), 419-425.

Kim, K. -C., Kim. K. Y., Park, Y. C., Jo, S. -H., Ryu, H. J., Yi, C. K., 2010. Study of hydrodynamics and reaction characteristics of K-based solid sorbents for $CO_2$ capture in a continuous system composed of two bubbling fluidized-bed reactors. Korean Chemical Engineering Research 48 (4), 499-505.

Kim, K. -C., Park, Y. C., Jo, S. -H., Yi, C. K., 2011. The effect of $CO_2$ or steam partial pressure in the regeneration of solid sorbents on the $CO_2$ capture efficiency in the two-interconnected bubbling fluidized-beds system. Korean Journal of Chemical Engineering 28 (10), 1986-1989.

Krutka, H., Sjostroma, S., Starnsa, T., Dillona, M., Silvermanb, R., 2013. Post-combustion $CO_2$ capture using solid sorbents: 1 MWe pilot evaluation. Energy Procedia 37, 73-88.

Lee, J. B., Ryu, C. K., Baek, J.-I., Lee, J. H., Eom, T. H., Kim, S. H., 2008. Sodium-based dry regenerable sorbent for carbon dioxide capture from power plant flue gas. Industrial and Engineering Chemistry Research 47 (13), 4465-4472.

Lee, S. C., Chae, H. J., Choi, B. Y., Jung, S. Y., Ryu, C. Y., Park, J. J., Baek, J. -I., Ryu, C. K., 2011. The effect of relative humidity on $CO_2$ capture capacity of potassium-based sorbents. Korean Journal of Chemical Engineering 28 (2), 480-486.

Liang, Y., Harrison, D. P., Gupta, R. P., Green, D. A., McMichael, W. J., 2004. Carbon dioxide capture using dry sodium-based sorbents. Energy & Fuels 18 (2), 569-575.

Mason, J. A., Sumida, K., Herm, Z. R., Krishna, R., Long, J. R., 2011. Evaluating metal−organic frameworks for post-combustion carbon dioxide capture via temperature swing adsorption. Energy & Environmental Science 4, 3030−3040.

Min, K., Choi, W., Kim, C., Choi, M., 2018. Oxidation-stable amine-containing adsorbents for carbon dioxide capture. Nature Communications 9, No. 726.

Min, K., Choi, W., Choi, M., 2017. Macroporous silica with thick framework for steam-stable and high-performance poly(ethyleneimine)/silica $CO_2$ adsorbent. ChemSusChem 10, 2518-2526.

Morris, W. J., Sjostrom, S., Sayyah, M., Denney, J., Syed, O., Lindsey, C., Lindsay, M., 2014. ADA's solid sorbent $CO_2$ capture process: developing solid sorbent technology to provide the necessary flexible $CO_2$ capture solutions for a wide range of applications. Energy Procedia 63, 1536-1545.

Nelson, T. O., Kataria, A., Mobley, P., Soukri, M., Tanthana, J., 2017. RTI's solid sorbent-based $CO_2$ capture process: technical and economic lessons learned for application in coal-fired, NGCC, and cement plants. Energy Procedia 114, 1536-1545.

Nguyen, T., Hilliard, M., Rochelle, G. T., 2010. Amine volatility in $CO_2$ capture. International Journal of Greenhouse Gas Control 4, 707-715.

Park, Y. C., Jo, S. -H., Bae, D. H., Min, B. M., Ryu, C. K., Yi, C. -K., 2014a. Development status of the $CO_2$ capture process with dual fluidized-beds for post-combustion CCS technology in Korea. Proceedings of the 13th International Conference on Clean Energy 1, 2730-2732.

Park, Y. C., Jo, S. -H., Kyung, D. -H., Kim, J. -Y., Yi, C. -K., Ryu, C. K., Shin, M. S., 2014b. Test operation results of the 10 MWe-scale dry-sorbent $CO_2$ capture process integrated with a real coal-fired power plant in Korea. Energy Procedia 63, 2261-2265.

Park, Y. C., Jo, S. -H., Lee, D. H., Yi, C. -K., Ryu, C. K., Kim, K. S., You, C. H., Park, K. S., 2013. The status of the development project for the 10 MWe-scale dry-sorbent carbon dioxide capture system to the real coal-fired power plant in Korea. Energy Procedia 37, 122-6.

Park, Y. C., Jo, S. -H., Lee S. -Y., Moon, J. -H., C. -K., Ryu, Lee, J. B., Yi, C. -K., 2016. Performance analysis of K-based KEP-CO2P1 solid sorbents in a bench-scale continuous dry-sorbent $CO_2$ capture process. Korean Journal of Chemical Engineering 33 (1), 73-79.

Park, Y. C., Jo, S. -H., Park, K. W., Park, Y. S., Yi, C. -K., 2009a. Effect of bed height on the carbon dioxide capture by carbonation/regeneration cyclic operations using dry potassium-based sorbents. Korean Journal of Chemical Engineering. 26, 874-878.

Park, Y. C., Jo, S. -H., Ryu, C. K., Yi, C. -K., 2009b. Long-term operation of carbon dioxide capture system from a real coal-fired flue gas using dry regenerable potassium-based sorbents. Energy Procedia 1, 1235-1239.

Park, Y. C., Jo, S. -H., Ryu, C. K., Yi, C. -K., 2011. Demonstration of pilot scale carbon dioxide capture system using dry regenerable sorbents to the real coal-fired power plant in Korea. Energy Procedia 4, 1508-1512.

Rochelle, G. T., 2009. Amine scrubbing for $CO_2$ capture. Science 325, 1652-1654.

Shang, J., Li, G., Singh, R., Gu, Q., Nairn, K. M., Bastow, T. J., Medhekar, N., Doherty, C. M., Hill, A. J., Liu, J. Z., Webley, P. A., 2012. Discriminative separation of gases by a ‘molecular trapdoor’ mechanism in chabazite zeolites. Journal of American Chemical Society 134, 19246–19253.

Wang, J., Huang, L., Yang, R., Zhang, Z., Wu, J., Gao, Y., Wang, Q., O’Hare, D., Zhong, Z., 2014. Recent advances in solid sorbents for $CO_2$ capture and new development trends. Energy & Environmental Science 7, 3478-3518.

White, C. M., Strazisar, B. R. Granite, E. J., Hoffman, J. S., Pennline, H. W., 2013. Separation and capture of $CO_2$ from large stationary sources and sequestration in geological formation-coalbeds and deep saline aquifers. Journal of the Air & Waste Management Association 53, 645-715.

Yi, C. -K., 2009. Advances of carbon capture technology. Korean Industrial Chemistry News 12(1), 30-42.

Yi, C. -K., 2010. Advances of post-combustion carbon capture technology by dry sorbent. Korean Chemical Engineering Research 48 (2), 140-146.

Yi, C. -K., Hong, S. W., Jo, S. -H., Son, J. E., Choi, J. H., 2005. Absorption and regeneration characteristics of a sorbent for fluidized-bed $CO_2$ removal process. Korean Chemical Engineering Research 43 (2), 294-298.

Yi, C. -K., Jo, S. -H., Seo, Y., 2008. The effect of voidage on the $CO_2$ sorption capacity of K-based sorbent in a dual circulating fluidized bed process. Journal of Chemical Engineering of Japan 41 (7), 691-694.

Yi, C. -K., Jo, S. -H., Seo, Y., Lee, J. B., Ryu, C. K., 2007. Continuous operation of the potassium-based dry sorbent $CO_2$ capture process with two fluidized-bed reactors. International Journal of Greenhouse Gas Control. 1 (1), 31-36.

Yi, C. -K., Jo, S. -H., Seo, Y., Moon, K. H., Yoo, J. S., 2006. $CO_2$ capture characteristics of dry sorbents in a fast fluidized reactor. Studies in Surface Science and Catalysis 159, 501-504.

Zhang, W., Liu, H., Sun, C., Drage, T. C., Snape, C. E., 2014. Performance of polyethyleneimine–

silica adsorbent for post-combustion $CO_2$ capture in a bubbling fluidized bed. Chemical Engineering Journal 251, 293–303.

Zhang, W., Liu, H., Sun, Y., Cakstins, J., Sun, C., Snape, C. E., 2016. Parametric study on the regeneration heat requirement of an amine-based solid adsorbent process for post-combustion carbon capture. Applied Energy 168, 394-405.

# List of Tables

**Table 1**

| | S.PEI-0.8K | S.PEI-5K |
|---|---|---|
| PEI molecular mass (g/mol) | 800 | 5000 |
| Bulk density (g/cm$^3$) | 0.5608 | 0.5512 |
| Average particle size (μm) | 230 | 240 |
| Particle distribution (μm) | 28 ~ 592 | 80 ~ 498 |
| Attrition index (%) | 3.27 | 2.09 |

**Table 2**

| Item | Adsorption reactor | Desorption reactor |
|---|---|---|
| Inlet flow rate (l/min) | 17.0 ~ 20.0 | 14.8 ~ 15.1 |
| Inlet $H_2O$ concentration (vol.%) | - | - |
| Inlet $CO_2$ concentration (vol.%) | 14.3 ~ 14.6 | - |
| Temperature ($^oC$) | 66 ~ 70 | 128 ~ 130 |
| Differential pressure (mm$H_2O$) | 280 ~ 300 | 280 ~ 300 |
| Inlet sorbent/$CO_2$ mass ratio at the adsorber (-) | 7.3 ~ 27.4 | |

**Table 3**

| Item | Adsorption reactor | Desorption reactor |
|---|---|---|
| Inlet flow rate (l/min) | 17.7 ~ 27.3 | 15.0 ~ 15.8 |
| Inlet $H_2O$ concentration (vol.%) | 3.0 ~ 7.1 | 0 ~ 4.5 |
| Inlet $CO_2$ concentration (vol.%) | 14.6 ~ 15.2 | - |
| Temperature (°C) | 56 ~ 66 | 119 ~ 130 |
| Differential pressure (mm$H_2O$) | 220 ~ 300 | 250 ~ 300 |
| Inlet sorbent/$CO_2$ mass ratio at the adsorber (-) | 11.2 ~ 15.2 | |

**Table 4**

| Item | Desorption reactor temperature (°C) | |
|---|---|---|
| | 119 ~ 120 | 129 ~ 130 |
| $CO_2$ removal efficiency (%) | 73.1 | 81.6 |
| Dynamic sorption capacity (wt.%) | 5.54 | 6.19 |

## List of Figures

Figure 1. Schematic diagram of the TBS.

Figure 2. The $CO_2$ removal efficiency and dynamic sorption capacity of S.PEI-0.8K adsorbent according to variation of inlet sorbent/$CO_2$ mass ratio at the adsorber (■ : $CO_2$ removal efficiency, □ : dynamic sorption capacity.

Figure 3. Results for the 180-hour continuous test in the TBS, (a) $CO_2$ removal efficiency and $CO_2$ concentration, (b) Dynamic sorption capacity and solid circulation rates, (c) $H_2O$ concentration, (d) Reactor temperature, (e) Differential pressure.

Figure 4. The $CO_2$ removal efficiency and dynamic sorption capacity of S.PEI-5K adsorbent according to variation of inlet sorbent/$CO_2$ mass ratio at the adsorber (■ : $CO_2$ removal efficiency, □ : dynamic sorption capacity).

Figure 5. Particle size distribution of silica-PEI sorbent (fresh and used), (a) Before and after the preliminarily test, (b) Before and after the 180-hour continuous test.

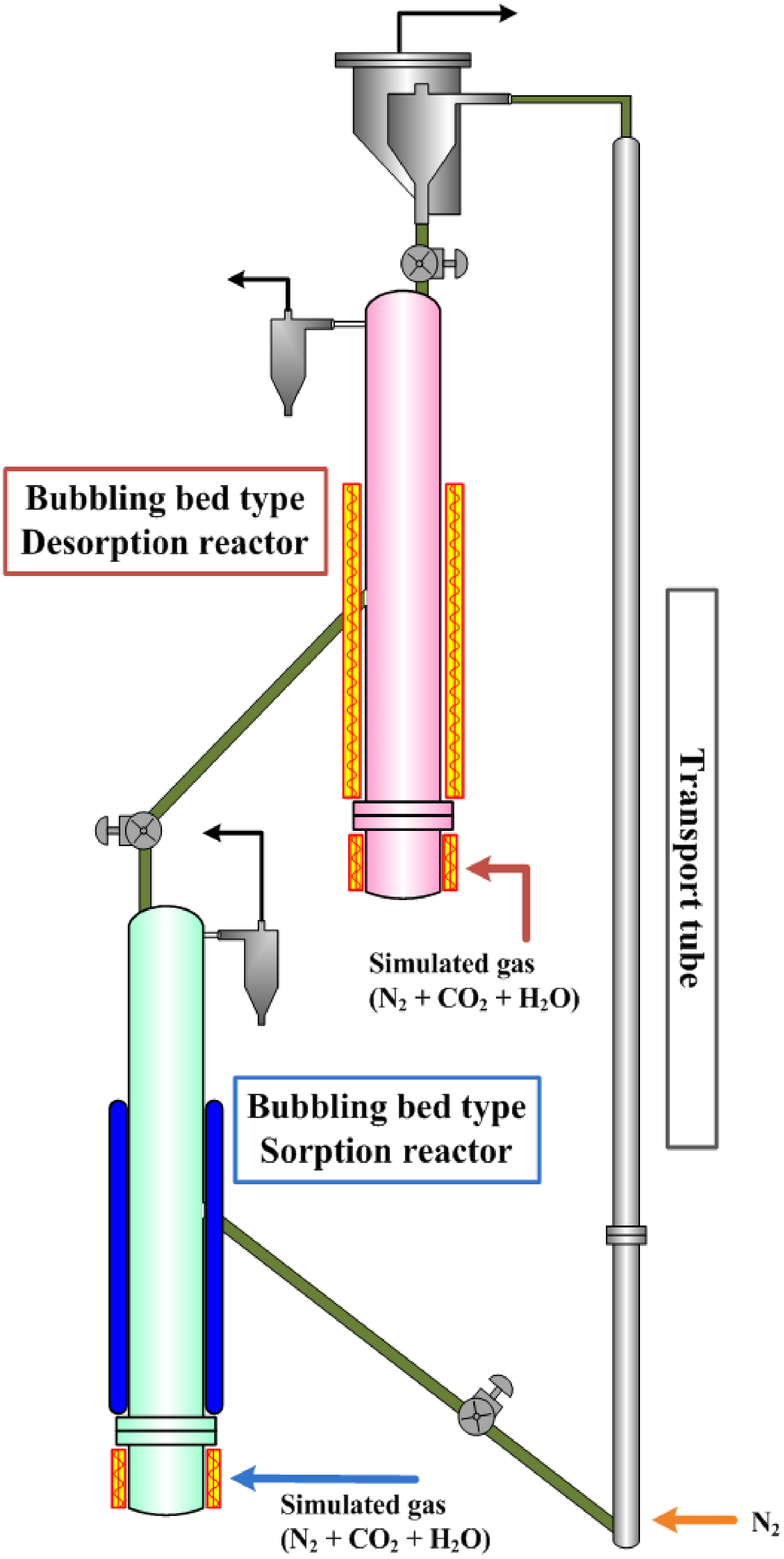
Bubbling bed type
Desorption reactor
Transport tube
Simulated gas
($N_2 + CO_2 + H_2O$)
Bubbling bed type
Sorption reactor
Simulated gas
($N_2 + CO_2 + H_2O$)
$N_2$

**Fig. 1.**

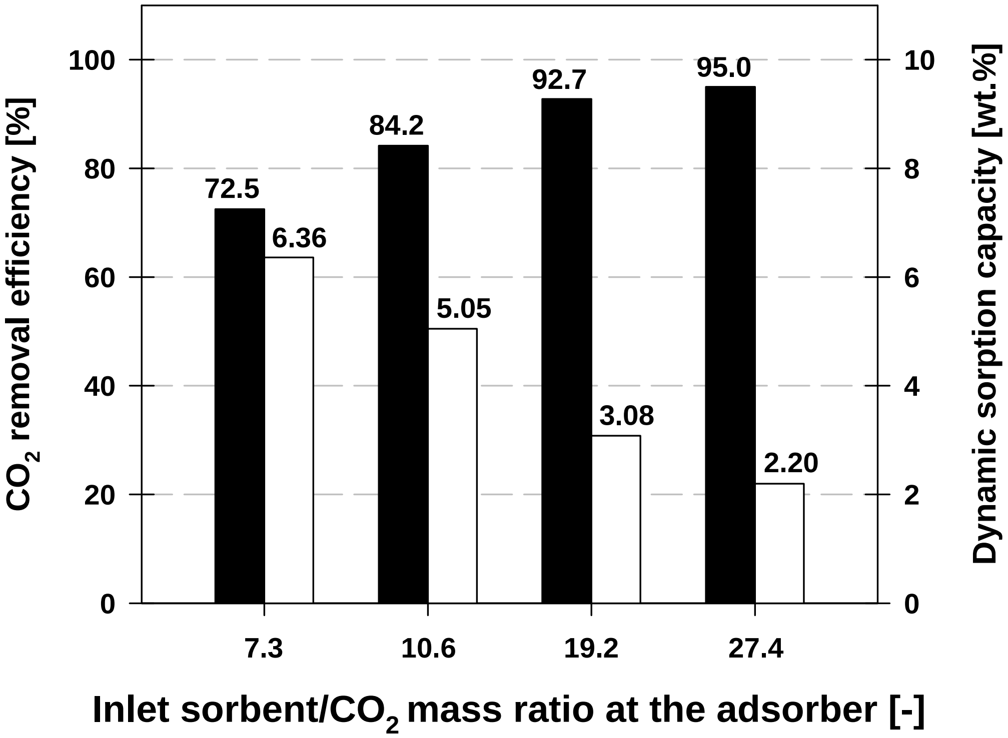
100
80
60
40
20
0
10
8
6
4
2
0
72.5
6.36
84.2
5.05
92.7
3.08
95.0
2.20
7.3
10.6
19.2
27.4
CO2 removal efficiency [%]
Dynamic sorption capacity [wt.%]
Inlet sorbent/CO2 mass ratio at the adsorber [-]

**Fig. 2.**

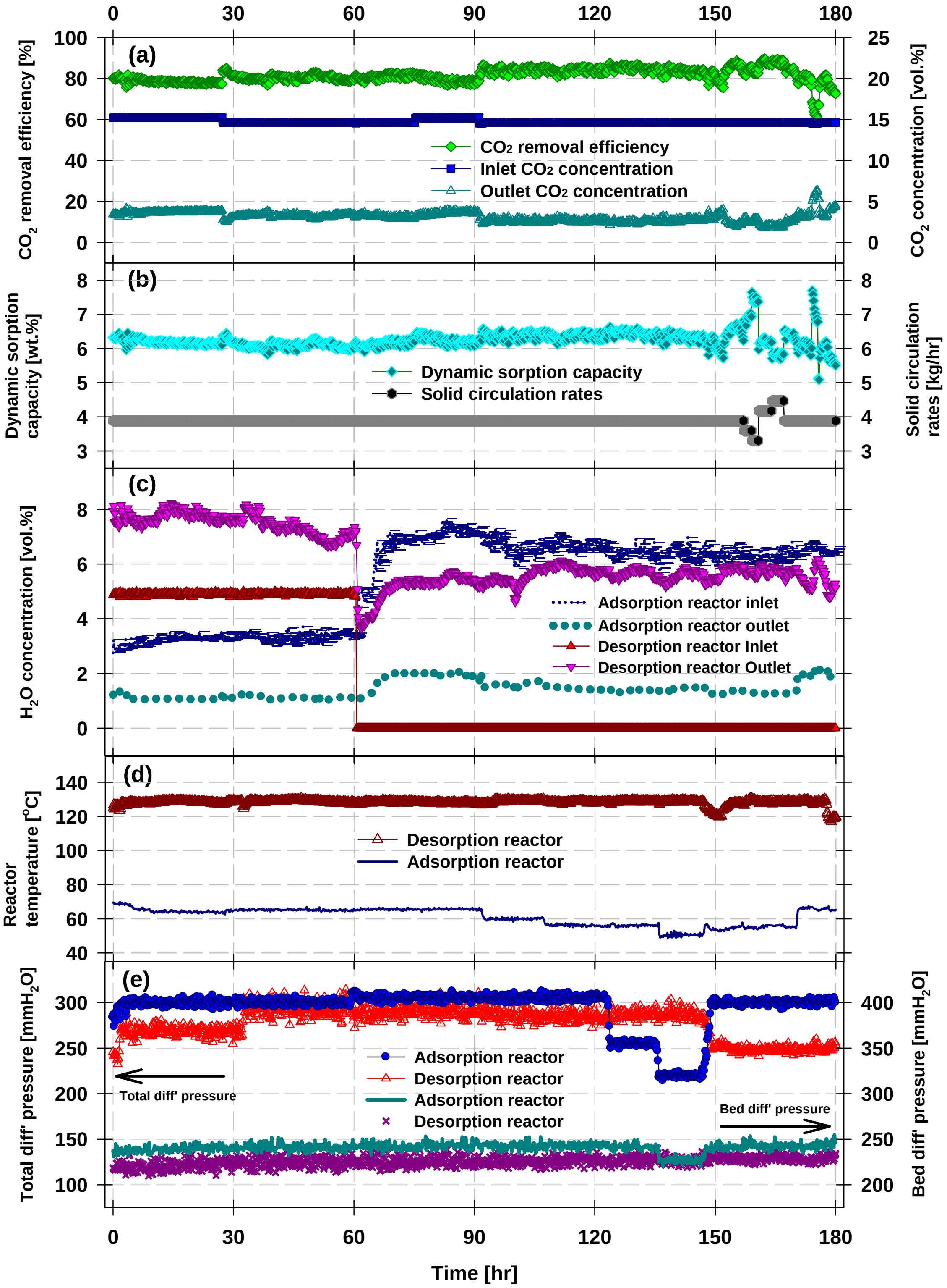

0
30
60
90
120
150
180
(a)
CO$_2$ removal efficiency [%]
100
80
60
40
20
0
CO$_2$ concentration [vol.%]
25
20
15
10
5
0
CO2 removal efficiency
Inlet CO2 concentration
Outlet CO2 concentration
(b)
Dynamic sorption capacity [wt.%]
8
7
6
5
4
3
Solid circulation rates [kg/hr]
Dynamic sorption capacity
Solid circulation rates
(c)
H$_2$O concentration [vol.%]
8
6
4
2
0
Adsorption reactor inlet
Adsorption reactor outlet
Desorption reactor Inlet
Desorption reactor Outlet
(d)
Reactor temperature [°C]
140
120
100
80
60
40
Desorption reactor
Adsorption reactor
(e)
Total diff' pressure [mmH$_2$O]
300
250
200
150
100
Bed diff' pressure [mmH$_2$O]
400
350
300
250
200
Adsorption reactor
Desorption reactor
Adsorption reactor
Desorption reactor
Total diff' pressure
Bed diff' pressure
Time [hr]

**Fig. 3.**

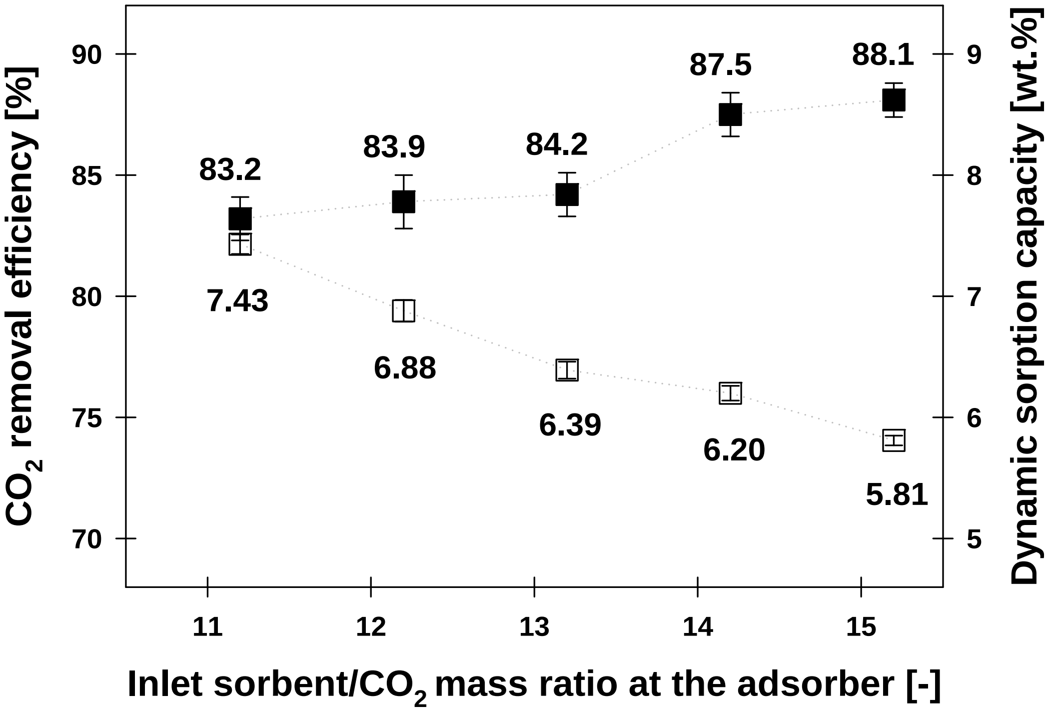
CO$_2$ removal efficiency [%]
90
85
80
75
70
Dynamic sorption capacity [wt.%]
9
8
7
6
5
11
12
13
14
15
Inlet sorbent/CO$_2$ mass ratio at the adsorber [-]
83.2
83.9
84.2
87.5
88.1
7.43
6.88
6.39
6.20
5.81

**Fig. 4.**

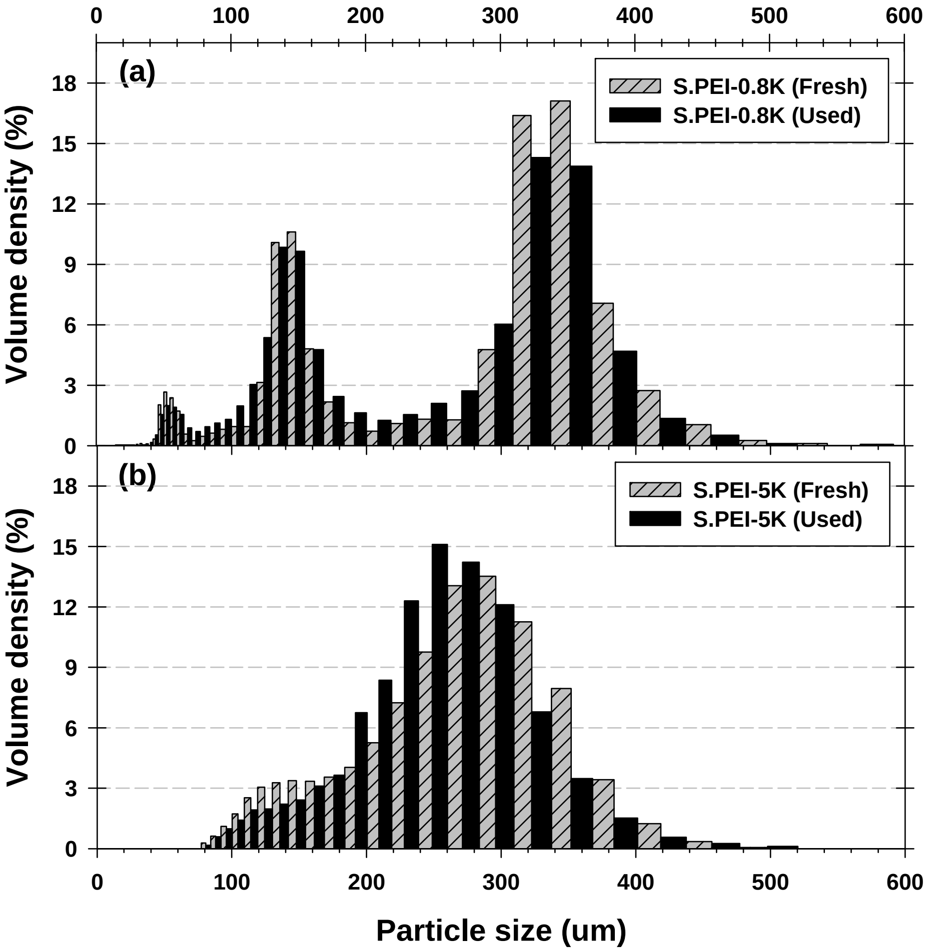

(a)
S.PEI-0.8K (Fresh)
S.PEI-0.8K (Used)
(b)
S.PEI-5K (Fresh)
S.PEI-5K (Used)
Volume density (%)
0
3
6
9
12
15
18
0
100
200
300
400
500
600
Particle size (um)

**Fig. 5.**